Effects of Non-Quartz Minerals in Natural Bed Sand on Agglomeration Characteristics during Fluidized Bed Combustion of Biomass Fuels

6 AUTHORS, INCLUDING:

Marcus Öhman
Luleå University of Technology
86 PUBLICATIONS **1,988** CITATIONS

SEE PROFILE

Dan Boström
Umeå University
136 PUBLICATIONS **1,982** CITATIONS

SEE PROFILE

Anders Nordin
Umeå University
66 PUBLICATIONS **1,714** CITATIONS

SEE PROFILE

Effects of Non-Quartz Minerals in Natural Bed Sand on Agglomeration Characteristics during Fluidized Bed Combustion of Biomass Fuels

Sigrid De Geyter,*,[†] Marcus Öhman,[‡] Dan Boström,[†] Morgan Eriksson,[§] and Anders Nordin[†]

Energy Technology and Thermal Process Chemistry, Umeå University, SE-901 87 Umeå, Sweden, Division of Energy Engineering, Luleå University of Technology, SE-971 87 Luleå, Sweden, and Övik Energi, Strandgatan 1, SE-891 33 Örnsköldsvik, Sweden

Most of the previous literature on fluidized bed agglomeration during biomass combustion is based on quartz as a bed material. Full-scale installations however often use natural sand, which apart from quartz may contain a high fraction of non-quartz minerals such as potassium feldspar and plagioclase. The objective of the present study was therefore to elucidate the effects of non-quartz minerals occurring in natural sand on the agglomeration behavior during fluidized bed combustion of biomass fuels. Three fuels typical for previously determined agglomeration mechanisms were chosen as model fuels: calcium-rich bark, potassium-rich olive residues, and silica- and potassium-rich wheat straw. Two different feldspar minerals were used: a potassium feldspar and a plagioclase, labradorite, which both occur in many commercial bed materials. Furthermore, olivine was used as a bed material as this mineral represents another type of bed material used in some full-scale installations. Quartz was used as a reference bed material. The effects of non-quartz minerals in natural sand on initial defluidization temperature were assessed during carefully controlled, bench-scale fluidized bed agglomeration experiments. Bed material samples and agglomerates were analyzed using scanning electron microscopy/energy-dispersive spectroscopy (SEM/EDS) in order to explore the occurrence and chemical composition of coating and attack layers on the bed particles and necks between agglomerated particles. Significant differences in agglomeration characteristics were found for the different minerals when bark and olive residue were combusted. Potassium-feldspar was shown to lower the initial defluidization temperature for combustion of bark and olive residues. Plagioclase and olivine on the other hand were found to increase the initial defluidization temperature as compared to quartz for the combustion of olive residue, but for bark combustion, they did not differ significantly from quartz. During combustion of wheat straw, all bed materials agglomerated shortly after the startup of the experiment. For bark and olive residue samples, attack layers were found on all bed materials and the composition of the inner attack layer and agglomerate necks differed significantly with the fuel/bed material combination. For wheat straw however, no continuous attack layers were found, and the bed material composition was concluded not to influence the agglomeration characteristics for this biomass. The results were used to suggest possible mechanisms involved in layer formation for the different minerals.

Introduction

Fluidized bed combustion has grown to become one of the most important technologies for combustion and gasification of biomass. In spite of many process advantages such as fuel flexibility and emission control, fluidized bed technology still suffers from the risk of agglomeration potentially resulting in total defluidization and unscheduled shutdown. Bed agglomeration phenomena during fluidized bed combustion of biomass have thus been subject to numerous studies. An extensive literature review on agglomeration mechanisms was compiled by Brus.[1] Coating and attack layer formation on the bed particles was pointed out as an important route for agglomeration/

defluidization of the fluidized bed combustion (FBC) of biomass fuels. A low melting temperature of this coating can result in agglomeration of the bed material.[2−6] The formation of a coating layer is a result of an interaction between the ash-forming elements in the fuel and the bed particles. In quartz beds, the

* Corresponding author. E-mail: sigrid.de.geyter@chem.umu.se.
† Umeå University.
‡ Luleå University of Technology.
§ Övik Energi.

(1) Brus, E. Bed agglomeration during combustion and gasification of biomass fuels-mechanisms and measures for prevention. Licenciate Thesis, Umeå University, Umeå, 2004; ISBN 91-7305-676-6.

(2) Visser, H. J. M.; van Lith, S.; Kiel, J. H. A. Agglomeration due to biomass ash-bed material interactions in fluidized bed reactors. In *12th European Conference on Biomass for Energy, Industry and Climate Protection*, Amsterdam, The Netherlands, June 17−21; Palz, W., Spitzer, J., Maniatis, K., Kwant, K., Helm, P., Grassi, A., Eds.; ETA-Florence: Florence, Italy, and Amsterdam, The Netherlands, 2002; pp 585−588.

(3) Benson, S. A.; Karner, F. R.; Goblirsch, G. M.; Brekke, D. W. Bed agglomerates formed by atmospheric fluidized bed combustion of a North Dakota lignite. *Prepr Pap−Am Chem Soc., Div Fuel Chem* **1982**, *27*, 174−181.

(4) Lin, W.; Krusholm, G.; Dam-Johansen, K.; Musahl, E.; Bank, L. Agglomeration phenomena in fluidized bed combustion of straw. In *Proceedings of the 14th International Conference on Fluidized Bed Combustion*. Vancouver, Canada, May 11−14; American Society of Mechanical Engineers: New York, 1997; pp 831−838.

(5) Manzoori, A. R.; Agarwal, P. K. Agglomeration and defluidization under simulated circulating fluidized-bed combustion conditions. *Fuel* **1994**, *73*, 563−568.

Table 1. Mineral Composition of Some Commercially used Bed Materials in Nordic Countries (in percent of particles)[10]

commercial name	quartz SiO_2 (%)	K-feldspar $KAlSi_3O_8$ (%)	plagioclase $(Ca, Na)Al_xSi_{4-x}O_8$ (%)	biotite mica $K(Mg, Fe)_3(OH, F)_2AlSi_3O_{10}$ (%)	other (%)
Baskarp 20	81.0	8.0	7.7	0.2	3.1
Råda 20	54.0	15.5	24.8	0.6	5.1

dominating mechanisms for agglomeration have been identified to be the following: (a) coating-induced agglomeration with attack and diffusion of calcium, forming low-melting silicates also including minor amounts of potassium, with subsequent viscous-flow sintering and agglomeration (typical for woody fuels), (b) direct attack by potassium in gas or aerosol phase, forming low-melting silicates inducing viscous-flow sintering and agglomeration (typical for alkali-rich fuels), and (c) direct adhesion by partly melted ash-derived potassium silicate particles/droplets (for fuels containing both potassium and high amounts of reactive silica).[7] Mechanisms a and b suggest that the bed material is playing an active role in the agglomeration process, whereas for mechanism c, the cause for agglomeration is found rather in the composition of the fuel ash. However, in several studies, the bed particle layers have been found to consist of several superimposed attack and coating layers.[6-9] The inner layers are rather homogeneous and grow inward by an attack or chemical reaction, whereas the outer layer is relatively inhomogeneous and consisting of small particles with a chemical composition resembling that of the fuel ash.[7]

However, most previous studies performed to elucidate the mechanisms involved in bed agglomeration during biomass combustion have used quartz as a bed material whereas full-scale installations more often use natural sand mixtures containing significant fractions of other minerals such as K-feldspars and plagioclases (Table 1).

In a previous study with a typical natural sand, a significantly lower agglomeration temperature for a potassium-rich fuel (olive residue) was obtained compared to pure quartz whereas a slight increase in agglomeration temperature with natural sand was found for bark combustion.[11] The objective of the present study was therefore to determine the effects of non-quartz minerals on agglomeration characteristics for the different types of previously identified bed agglomeration mechanisms.

Experimental Section

Bed Materials and Fuels. Bed materials were chosen based on their relevance for full-scale installations in Nordic countries.

Feldspars are a very large group of minerals constituting about half of the earth crust. They are aluminum silicates with either potassium or varying levels of calcium and sodium. Two types of

(6) Öhman, M.; Nordin, A.; Skrifvars, B.-J.; Backman, R.; Hupa, M. Bed Agglomeration Characteristics during Fluidized Bed Combustion of Biomass Fuels. *Energy Fuels* **2000**, *14* (1), 169−178.

(7) Brus, E.; Öhman, M.; Nordin, A. Mechanisms of bed agglomeration during fluidized-bed combustion of biomass fuels. *Energy Fuels* **2005**, *19* (3), 825−832.

(8) Latva-Somppi, J.; Kauppinen, E. I.; Valmari, T.; Ahonen, P.; Burav, A. S.; Kodas, T. T.; Johanson, B. The ash formation during co-combustion of wood and sludge in industrial fluidized bed boilers. *Fuel Process. Technol.* **1998**, *54*, 79−94.

(9) Nuutinen, L. H.; Tiainen, M. S.; Virtanen, M. E.; Enestam, S. H.; Laitinen, R. S. Coating Layers on Bed Particles during Biomass Fuel Combustion in Fluidized-Bed Boilers. *Energy Fuels* **2004**, *18* (1), 127−139.

(10) Östlin, D. *Provning av svenska gjuterisanders egenskaper*; 830114, Svenska Gjuteriföreningen (www.gjuteriforeningen.se): Sweden, 1983.

(11) De Geyter, S.; Öhman, M.; Eriksson, M.; Boström, D.; Berg, M. Agglomeration characteristics using alternative bed materials for combustion of biomass. In *14th European Biomass Conference-Biomass for Energy, Industry and Climate Protection*, Paris, France, Oct 17−21; ETA-Florence: Florence, Italy, and Paris, France, 2005.

Table 2. Bed Material Elemental Composition According to Suppliers Specifications or Scanning Electron Microscopy/Energy-Dispersive Spectroscopy (SEM/EDS) Analysis

oxide	quartz (wt %)	plagioclase[a] (wt %)	K-feldspar (wt %)	olivine (wt %)
SiO_2	98.9	54	66.2	45.05
Al_2O_3	0.181	27	19.3	0.45
Fe_2O_3	0.123		0.1	7.05
CaO	0.123	11	1.3	0.075
MgO	0.129		0.1	49.5
Na_2O	0.004	6	4.8	
K_2O	0.060		8.2	
MnO	0.013		0.075	
P_2O_5	<0.012		0.12	
TiO_2	0.040			
Cr_2O_3			0.25	
NiO			0.325	
Rb_2O			0.07	0.07

a Scanning electron microscopy/energy-dispersive spectroscopy (SEM/EDS) analysis.

Table 3. Fuel Characteristics (Elemental Composition)

	bark	olive residue	wheat straw
dry substance (wt % of fuel)	90.6	85.1	91.6
ash content (wt % of ds[a])	3.0	6.6	7.1
Cl (wt % of ds[a])	0.01	0.09	0.25
S (wt % of ds[a])	0.03	0.1	0.11
Ash Elements (wt % of Ash)			
SiO_2	14.6	16.1	57.8
Al_2O_3	2.24	2.59	1.0
CaO	38.7	13.6	10.4
Fe_2O_3	<3.9	1.8	0.3
K_2O	7.7	33.0	12.5
MgO	3.6	5.2	1.9
MnO	1.5	0.05	
Na_2O	<1.6	0.7	0.6
P_2O_5	2.84	4.35	3.3
TiO_2	0.1	0.1	0.1

a ds: dry substance.

feldspars, both dominating the non-quartz mineral content of natural sand, were tested separately: potassium-feldspar and plagioclase. Table 2 gives an overview of the elemental composition of the different bed materials. X-ray diffraction analysis (XRD) revealed the crystal phases present in the bed material samples. The potassium feldspar bed material consisted mainly of $K_{0.94}Na_{0.06}AlSi_3O_8$ with some traces of albite ($NaAlSi_3O_8$). The plagioclase bed material used in the experiments consisted of labradorite ($Na_{0.4}Ca_{0.6}Al_{1.6}Si_{2.4}O_8$). Another mineral that often appears in commercial bed materials is olivine. According to XRD analysis, the olivine used in the experiments was approximately $Mg_{1.8}Fe_{0.2}SiO_4$.

Fuel types were chosen based on the different types of agglomeration mechanisms previously identified in quartz.[7] Bark was used to represent woody fuels which typically have a high calcium content and follow mechanism a. For mechanism b, a potassium-rich olive residue was chosen. Wheat straw was used to represent agricultural residues with high potassium and silica content (mechanism c). The fuel compositions are summarized in Table 3.

The bed materials were standardized by sieving to 125−150 μm in order to eliminate the possible effects of different particle sizes. A total of 540 g of bed material was used for each experiment.

Combustion and Agglomeration Experiments. The controlled fluidized bed agglomeration (CFBA) method, described in detail

elsewhere,[12] was used for the combustion and agglomeration experiments. The bench-scale bubbling fluidized bed (BFB) reactor consisted of a 2 m high stainless steel tube, with a bed section and freeboard diameters of 100 and 200 mm, respectively. Primary or fluidization air was injected through a perforated plate with 1% open area. The air flow was set to 40 L/min. For each combustion experiment, the reactor was first heated by external wall heating elements and heated primary air. The bed material was introduced gradually during the heating up of the reactor and fluidized at all times. When the desirable bed temperature was reached, the pelletized model fuels were introduced into the BFB reactor by a speed-controlled rotating fuel feeder and combusted continuously and separately for 40 h or until agglomeration occurred. A bed temperature of 760 °C for olive residue and wheat straw and 800 °C for bark and an oxygen concentration of 6% in the flue gases were maintained and controlled throughout the experiments. The lower combustion temperatures for olive residue and wheat straw were chosen to minimize the risk for direct agglomeration during the combustion stage. After 40 h of combustion, the fuel feeding was stopped and temperature staging was started by external heating. Combustion of propane gas was started to maintain a combustion atmosphere in the reactor while the bed was heated continuously and isothermally at 3 °C/min until bed agglomeration was achieved or until the maximum allowed temperature of 1050 °C was reached.

The onset of defluidization in the CFBA method is indicated by a drop in differential bed pressures and deviations in the bed temperature measurements registered continuously. The reproducibility of measuring the initial defluidization temperature with this method has previously[12] been determined to be ±5 °C.

SEM/EDS Analysis. Bed samples taken at the end of the combustion period (40 h) prior to the temperature staging phase as well as after agglomeration were mounted in epoxy, cut, and polished. Scanning electron microscopy/energy-dispersive spectroscopy (SEM/EDS) was then used to examine cross sections of particles and agglomerate necks for their morphology and elemental composition. A total of four or five particles were analyzed for each sample and five spots evenly distributed over the bed particle's periphery were chosen for elemental analysis and estimation of layer thickness. Albite particles found in K-feldspar bed material samples were evaluated separately. Where bed particle layers were found, inner attack and outer coating layers were analyzed separately. Inner attack and outer coating layers were discerned visually on the SEM image of the cross sections, and spots for elemental analysis were chosen in the middle of each layer. Where the layers were thin, influence of the bed material on the analysis results cannot be totally excluded due to the limited spatial resolution for quantification with SEM/EDS (a few micrometers). For agglomerate necks, at least 20 spots were chosen for elemental analysis.

Chemical Equilibrium Calculations. Chemical equilibrium model calculations with FactSage together with data from the FACT database[13] were used to interpret the results. The main elements constituting bed particle layers together with the components of a typical combustion atmosphere were used as input elements.

Results

Controlled Fluidized Bed Agglomeration Experiments. The results of the bench-scale agglomeration experiments with bark and olive residue are summarized in Table 4. Wheat straw caused all bed materials to agglomerate within the first 2 h of the combustion stage.

The documented range between initial defluidization and total agglomeration temperature is given as the CFBA agglomeration

(12) Öhman, M.; Nordin, A. A New Method for Quantification of Fluidized Bed Agglomeration Tendencies: A Sensitivity Analysis. *Energy Fuels* **1998**, *12*, 90–94.

(13) Bale, C. W.; Chartrand, P.; Degterov, S. A.; Eriksson, G.; Hack, K.; Ben Mahfoud, R.; Melancon, J.; Pelton, A. D.; Petersen, S. FactSage Thermochemical Software and Databases. *CalPhad* **2002**, *26* (2), 189–228.

Table 4. Summary of the Results: Initial Defluidization Temperature According to CFBA Experiments, Dominating Elements in Agglomerate Necks (SEM/EDS), and the Corresponding Theoretical Initial Melting Temperatures According to Relevant Ternary Phase Diagrams[h]

	CFBA aggl temp (°C)	dominating neck elements	theoretical initial melting temp (°C)
		Bark	
quartz	980–1000[a]	Si, K, Ca	750[c]
K-feldspar	865–875	Si, K, Al	710[d]
plagioclase	980–1040	Si, Ca, Al	1170[e]
olivine	960–990	Si, Mg, K	1050[f]
		Olive Residue	
quartz	(21.5 h)[b]	Si, K, Ca	725[c]
K-feldspar	(5.5 h)[b]	Si, K, Na	540[g]
plagioclase	845–855	Si, K, Ca	840[c]
olivine	755–765	Si, K, Mg	905[f]

[a] Brus et al.[14] [b] Agglomeration occurred during the combustion phase (*time of combustion prior to defluidization*). [c] Morey et al.[15] [d] Osborn and Muan.[16] [e] Osborn and Muan.[17] [f] Roedder.[18] [g] Kracek.[19] [h] Compositions are found from Figure 3.
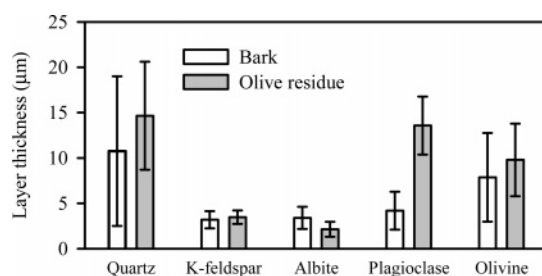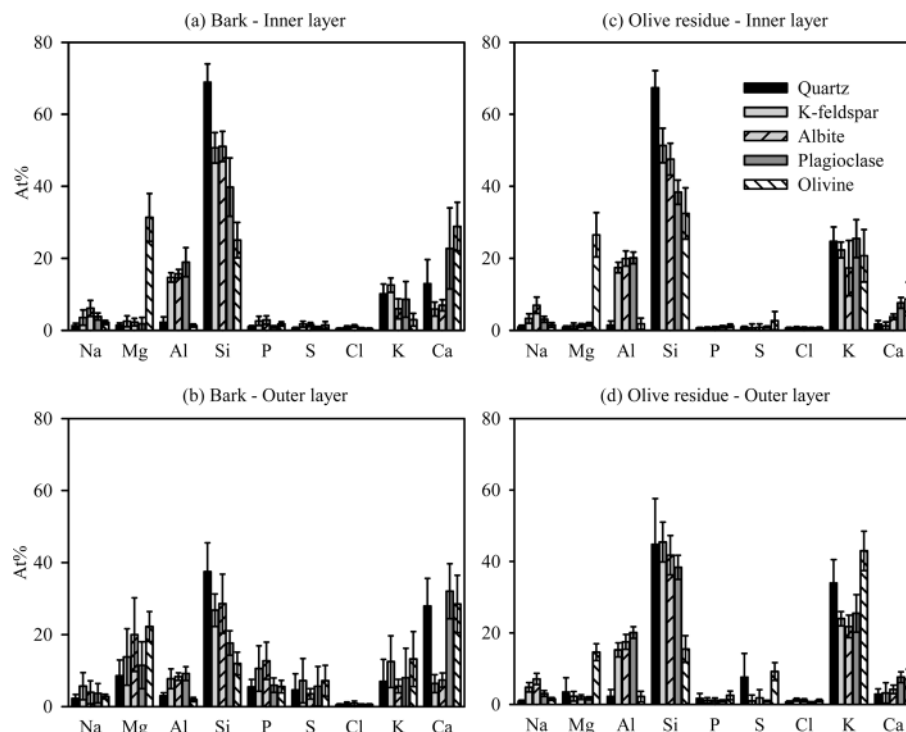

Figure 1. Total bed particle layer thickness.

temperature in Table 4. The results indicate that there are significant differences in agglomeration behavior between the different minerals in natural sand for combustion of bark and olive residue. K-feldspar is found to reduce the initial defluidization temperature compared to the other bed materials. Plagioclase indicated a small tendency to increase the initial defluidization temperature for bark compared with quartz. For olive residue, plagioclase significantly increases the initial defluidization temperature by about 100 °C and agglomeration occurred during temperature staging after a fully completed combustion stage. Olivine does not influence the initial defluidization temperature for bark significantly when compared to quartz, but olive residue could be combusted for 40 h as compared to 21.5 h for quartz.

SEM/EDS Analysis. Combustion of wheat straw did not result in coating formation on the bed particles and only some scarce agglomerate necks were found. This may be due to the very short combustion period (less than 2 h) prior to agglomeration. If present, the scarce layers were discontinuous and resembled spots of sticky residual ash particles instead of continuous attack layers. Agglomerate neck compositions were dominated by Si and K although some Mg and Ca were enriched for olivine and plagioclase, respectively. For K-feldspar and wheat straw, no necks were found at all.

Bark and olive residue combustion resulted in continuous layers on the bed particles for all bed materials. The inner attack layer was rather homogeneous whereas the outer coating layer had a more granular structure. K-feldspar and albite had very thin layers for both bark and olive residue combustion (Figure 1). A thin layer may be an effect of the much shorter combustion period prior to agglomeration in the case of olive residue but can also be an effect of a limited interaction potential between fuel-ash alkali with the K-feldspar and albite particles. Because of the thinner layers, effects due to limited spatial resolution

Figure 2. Elemental analysis of inner attack (a and c) and outer coating (b and d) layers upon combustion of bark (a and b) and olive residue (c and d).

could in these cases not be excluded during elemental analysis with SEM/EDS.

The elemental composition of inner attack and outer coating layers is shown in Figure 2a−d.

For bark combustion, inner layers of K-feldspar, albite, and plagioclases differ from quartz by having significantly lower Si and higher Al contents. Inner layers for olivine have significantly lower Si and K and higher Ca and Mg contents than quartz, whereas K-feldspar and albite tend to contain less Ca.

Also for olive residue, the inner layers for K-feldspar, albite, and plagioclase contain more Al and less Si than for quartz, whereas olivine is enriched in Mg and Ca. Plagioclase also contains significantly more Ca than quartz.

The outer layers of the bed materials for the different biomass fuels differ generally from the inner layers by having a larger variation in elemental composition and further enrichment with ash forming elements in the fuel. For K-feldspar and albite particles, a comparatively low Ca content was found for Ca-rich bark combustion.

Because of the limited spatial resolution of the SEM/EDS analysis, influences of the adjacent layers are difficult to exclude when layer thicknesses are small. It is therefore often difficult to conclude whether there has been a chemical interaction between the bed material and the fuel ash. For the much wider agglomerate necks, however, border effects are less important.

Agglomerate neck compositions (Figure 3) are similar to the inner attack layers for bark. Less K and more Al is however found in the agglomerate necks for K-feldspar and plagioclase as compared to quartz. K-feldspar necks further differ from quartz by a lower Ca content. For olive residue, olivine has a lower Si and a higher K and Mg content than quartz whereas K-feldspar necks contain more Al and Na and less K. Plagioclase differs from quartz by having more Ca and Al and less Si in the agglomerate necks.
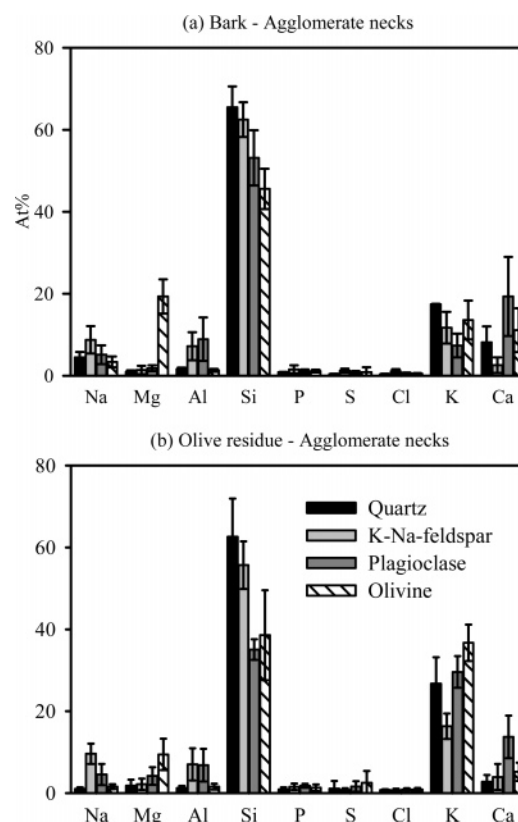

Figure 3. Elemental analysis of the agglomerate necks upon combustion of bark (a) and olive residue (b).

Discussion

For wheat straw, no differences were found in the agglomeration characteristics for the different bed materials. Almost no layers were found on the bed particles and agglomeration occurred within 2 h from the start of wheat straw combustion. The analysis of the scarce agglomerate necks revealed some

influence of the bed materials, but agglomeration occurred most probably because of a high amount of sticky potassium silicate ash particles in the bed area. This confirms the assumption that wheat straw follows mechanism c which was described as direct adhesion to the bed particles of partly melted ash derived potassium silicate particles,[7] thus with very limited interaction with bed materials. This is also consistent with previous studies with wheat straw and blast furnace slag.[14]

For the other fuels, the CFBA experiments revealed significant differences in the agglomeration tendencies between quartz and different non-quartz minerals when tested as bed materials. Layers were found to differ in composition and thickness for the different bed materials upon combustion of bark and olive residue. As the formation of a layer has often been found to initiate agglomeration for quartz-based bed materials in earlier studies, an attempt is made here to interpret the results of the current study with regard to the mechanisms involved in layer formation on non-quartz minerals for these biofuels. On the basis of the observed elemental composition of the formed layers and chemical equilibrium model calculations, responsible chemical driving forces for bed layer formation are suggested below.

Layer Formation. In general, it is found that potassium plays a key role in bed particle layer formation as well as in bed agglomeration. It is also well-known that interaction of potassium with silica is highly dependent on the degree of silicate polymerization. Highly polymerized melted silicate structures accommodate alkali metal cations like potassium more easily in large cavities in their Si tetrahedral network, than the disilicate or orthosilicate structures typically found in wood ash melts, where bond distances are smaller, allowing only for smaller alkaline earth elements.[20] This is also reflected by the general results of the chemical equilibrium calculations.

For quartz, presumably a highly polymerized potassium-silicate melt is formed on the bed particle surfaces by gaseous attack of alkali and/or melted potassium silicate particles. If Ca is available in the fuel (e.g. bark), this layer grows and gradually incorporates Ca as it reacts with CaO. The silicate layer thus formed increasingly "protects" the particle from further potassium attack, as it becomes more and more depolymerised.

Starting from K-feldspar and for increasing levels of potassium (gaseous attack), the initial melting temperatures might be about 100 deg higher than for quartz.[16] This temperature might be too high for any substantial amount of melt to be formed. Still, melted potassium silicate from surrounding ash may adhere to the feldspar particles. This melt will probably be in equilibrium with the feldspar together with solid potassium silicates.[13] Because of this lack of chemical driving force, no substantial layer-forming reaction will take place involving feldspar, which may explain the relatively small bed particle layer thickness for K-feldspar. On the other hand, lower initial defluidization temperatures were found for K-feldspar. A

possible explanation is that more potassium-silicate melt was retained in the ash as a consequence of the low degree of layer formation, inducing agglomeration following a mechanism of type c as described earlier.

Plagioclase developed thin bed particle coatings during bark combustion but relatively thick layers during olive residue combustion. Tentatively, a reaction between the plagioclase surface and gaseous potassium species will move the composition of the former toward an assembly comprising gehlenite ($Ca_2Al_2SiO_7$), leucite ($KAlSi_2O_6$), and alumina (Al_2O_3), whereas the reaction with melted potassium silicate will produce leucite and wollastonite ($CaSiO_3$).[21] The high agglomeration temperatures of plagioclase bed particles are probably a function of the ability of "neutralizing" gaseous potassium species and potassium-silicate melt by forming the relatively refractive leucite. No melt is produced in these reactions. This reasoning is based solely on the dominating anortite component ($CaAl_2Si_2O_8$) in the plagioclase. The albite ($NaAlSi_3O_8$) component is assumed to behave analogously to K-feldspar.

Similarly, when olivine is present, a reaction between gaseous potassium and the olivine surface is plausible. Several K-Mg-silicates exist that are conceivably products of such a reaction.[18] Moreover, melted potassium silicate from surrounding ash may adhere to the olivine surface and react with the K-Mg-silicates. When bark is combusted, the melted potassium-silicate ash particles will be relatively rich in Ca, able to react with the olivine (Mg_2SiO_4) surface to form monticellite ($MgCaSiO_4$).

Agglomerate Neck Composition. By drastically simplifying the multicomponent situation found in agglomerate necks to only focus on the main three elements, further understanding of the agglomeration characteristics may now be gained from consulting ternary equilibrium phase diagrams. The theoretical initial melting temperatures thus found for the main elements in the agglomerate necks are summarized in Table 4 and reveal similar trends as found from the CFBA experiments.

Three out of eight of the bed material/fuel combinations resulted in agglomerate neck compositions with main components in the $K_2O-CaO-SiO_2$ system. In this system, the Ca/K ratio is particularly interesting since a higher Ca content results in approaching a region with a high first peritectic (1075 °C, high Ca side), whereas increasing the K concentration moves the composition toward a region with a low eutectic (725 °C, high K side), illustrating the effect of increased initial melting temperatures by introducing Ca into a potassium silicate (e.g., suspended or adhered ash particles). Another way of increasing the initial melting temperature in this system is to lower the amount of Si, illustrated clearly by the plagioclase—olive residue case.[15]

Combustion of bark in a K-feldspar bed resulted in agglomerate necks with Si, K, and Al as dominating elements. Introduction of Al into a potassium silicate melt lowers the melting temperatures at least for high K/Al and low (K_2+Al_2)/Si ratios where eutectics as low as 695 °C occur.[16]

For agglomerate necks containing Ca together with Si and Al (Plagioclase-bark), no melting temperatures in this system are lower than 1170 °C.[17]

The introduction of Na into a potassium silicate, which occurred for K-feldspar in combination with olive residue, will lead to severe decreases in initial defluidization temperatures, the theoretical melting points being as low as 540 °C.[19] This was also found by Blander and Pelton.[22]

(14) Brus, E.; Öhman, M.; Nordin, A.; Bostrom, D.; Hedman, H.; Eklund, A. Bed agglomeration characteristics of biomass fuels using blast-furnace slag as bed material. *Energy Fuels* **2004**, *18* (4), 1187−1193.

(15) Morey, G. W.; Kracek, F. C.; Bowen, N. L. The ternary system of K2O-CaO-SiO2. *J. Soc. Glass Technol.* **1931**, *14*, 149−187.

(16) Levin, E. M.; Robins, C. R.; McMurdie, H. F. *Phase Diagrams for Ceramists*; American Ceramic Society: Columbus, OH, 1964; p 156, Figure 407.

(17) Levin, E. M.; Robins, C. R.; McMurdie, H. F. *Phase Diagrams for Ceramists*; American Ceramic Society: Columbus, OH, 1964; p 219, Figure 630.

(18) Roedder, E. W. The system K2O−MgO−SiO2, Part 1. *Am. J. Sci.* **1951**, *249*, 97−130.

(19) Kracek, F. C. The ternary system K2SiO3−Na2SiO3−SiO2. *J. Phys. Chem.* **1932**, *36*, 2529.

(20) Thy, P.; Lesher, C. E.; Jenkins, B. M. Experimental determination of high-temperature elemental losses from biomass slag. *Fuel* **2000**, *79* (6), 693−700.

(21) Roth, R. S.; Dennis, J. R.; McMurdie, H. F. *Phase Diagrams for Ceramists*; American Ceramic Society: Westerville, OH, 1987; p 476, Figure 6931.

(22) Blander, M.; Pelton, A. D. The inorganic chemistry of the combustion of wheat straw. *Biomass Bioenergy* **1997**, *12* (4), 295−298.

Where Mg was present in the agglomerate necks (olivine), positive effects were seen on the initial defluidization temperatures. The lowest eutectic temperatures in the $K_2O-MgO-SiO_2$ diagram are found for pure potassium silicates. Small increases of Mg in potassium silicate can induce large differences in the initial melting temperatures,[18] since low levels of Mg (some weight percent) are able to remove the composition toward regions controlled by higher eutectic temperatures.

Conclusions

• The K- and Si-rich wheat straw agglomeration was not influenced by the bed material. The wheat straw ash itself melted causing the bed to agglomerate even before any layers had time to develop.

• Different minerals in natural sand influence the agglomeration characteristics for Ca-rich bark and K-rich olive residue differently compared to quartz:

  ○ Plagioclase increased the initial defluidization temperature, significantly for olive residues but not significantly for bark. A tentative explanation is the ability of the anortite component in plagioclase to form leucite in reaction with fuel potassium.

  ○ Olivine increased the combustion time prior to agglomeration for olive residue but had no significant effect on initial defluidization temperature during bark combustion. Mg increases melting temperatures of pure potassium silicate.

  ○ K-feldspars worsened the agglomeration risk for both bark and olive residues significantly. Introduction of Al into a potassium silicate melt lowers the melting temperatures for high K/Al and low (K_2+Al_2)/Si ratios.

In general, minerals in natural sand are found to react differently from quartz in fluidized bed combustion of biomass fuels and their reaction depends on the fuel ash composition. A straightforward recommendation for the use of natural sand as a bed material in fluidized bed combustion is therefore difficult to make. A better understanding of potential mechanisms involved in bed agglomeration is however gained by studying non-quartz bed materials.